Natural As–Sb alloys: texture types, thermal behaviour and mechanism of formation

G. P. BERNARDINI,[1] C. CIPRIANI,[2] F. CORSINI,[1] G. G. T. GUARINI,[3] G. MAZZETTI[2] AND L. POGGI[1]

[1]Department of Earth Sciences, [2]Mineralogical Museum and [3]Department of Chemistry of the University of Florence, I-50121 Florence, Italy

Abstract

The thermal behaviour and mechanism of formation of different texture types of intergrown As–Sb alloys have been studied by DTA and annealing experiments performed on natural samples. The constant composition of the As-rich component and of the stibarsen in the intergrowths, and the large compositional range of the homogeneous solid solution obtained after heating in the DTA cycle, have been established using the linear relationship between cell volume and composition. The high-temperature features detected in the DTA studies of the natural samples confirm previously published phase relations for the synthetic As–Sb system. The low-temperature features can be correlated with the homogenization reaction which leads to the formation of a complete solid solution. Study of TTT plots based on the annealing experiments clearly shows that a diffusion mechanism is involved in the homogenization reaction. This has been further substantiated by fitting the experimental data to kinetic equations for diffusion-controlled processes. The kinetic parameters evaluated from the ending time for the 520, 480, and 420 °C annealing experiments, using both the Arrhenius and the transition state theory formalisms, suggests a rather rigid activated complex for the rate-determining step of the process.

KEYWORDS: arsenic, antimony, alloys, thermal analysis.

Introduction

NATURAL associations in the As–Sb system include that of metallic As or Sb with the intermetallic compound stibarsen (SbAs) (commonly referred to as 'allemontite'—Wretblad, 1941). Paradocrasite (Sb_3As) (Leonard *et al.*, 1971) is also known in nature.

Natural As–Sb associations (see Bernardini *et al.*, 1984) show characteristic textures classified by Ramdohr (1980) on the basis of the physical state of the high-temperature phase from which they are supposed to derive. The most typical of these textures are the As 'scherbenkobalt', with vermiform veinings of stibarsen, and the eutectoidic texture (myrmekitic) between As and stibarsen. It is possible, however, to observe in the natural samples a whole series of intermediate textures from the As-scherbenkobalt to the homogeneous stibarsen and paradocrasite.

In the synthetic As–Sb system (Skinner, 1965) below the solidus curve, which shows a minimum at 605 °C and the composition Sb 80 at.%, there is a complete solid solution down to room temperature. No solvus curve which could account for the textures observed in natural samples is observed. Wretblad (1941), in his study on the minerals of the Varuträsk pegmatite, suggested that the presence of minor elements may catalyse the exsolution process.

Skinner (1965), in his review of the literature pertaining to the phase relations in the As–Sb system starting with the work of Parravano and De Cesaris (1912), shed some doubt on the existence of the cubic compound found by Trzebiatowsky and Bryjac (1938) in their X-ray study of the As–Sb system. While Trzebiatowsky (1939) rejected Wretblad's (1939) suggestion that the cubic compound is, in fact, a solid solution between As_2O_3 and Sb_2O_3, Skinner (1965) also was unable to reproduce such a cubic phase. Groncharov *et al.* (1977) suggested, on the basis of thermodynamic calculation, a possible unmixing of the high-temperature solid solution with decreasing temperature. Bernardini *et al.* (1984) performed some experiments on synthetic samples containing traces of uranium which indicated the beginning of an exsolution process. However, the presence of a solvus (or solvi)

Mineralogical Magazine, June 1987, Vol. 51, pp. 295–304

at low temperature was not confirmed. It seemed worthwhile, therefore, to investigate the thermal behaviour of several types of As–Sb alloy associations using both heating and isothermal experiments, in order to understand the processes leading to the textural features observed in natural samples.

Methods of experimental investigation

Samples labelled 'allemontite' from different localities were kindly provided by many Italian Mineralogical Museums and were investigated by X-ray diffraction and reflected light microscopy. Also, high-temperature X-ray analyses were performed using evacuated silica glass capillaries in a Rigaku–Denky Debye camera and high-temperature optical investigations were carried out with a Leitz 1350 heating stage in a nitrogen atmosphere.

The thermal behaviour was investigated by DTA using a Mettler TA 2000C thermoanalyser at a heating rate of 5 °C/min., employing a modified form of Kullerud's (1971) technique, with flat-bottom silica glass vials and Al_2O_3 powder. Isothermal experiments were performed by annealing both small fragments of one sample at 150, 250, 350, 450 and 570 °C, for periods ranging from 20 min. to 4 weeks, and individual charges of 100 mg of powdered sample, at temperatures of 420, 450, 480 and 520 °C, for periods ranging from 5 to 600 min., in horizontally heated nichrome-wound furnaces.

Lattice parameters of the phases As, Sb and stibarsen, and of the (As,Sb) solid solutions obtained as the result of the DTA runs on the different types, were determined using a Philips PW 1130/90 diffractometer with Co-$K\alpha$ radiation at a scan speed of $\frac{1}{4}°$ 2θ/min. and a chart speed of 10 mm/min. X-ray measurements were taken at 25 °C, the 003, 014 and 110 reflections being measured relative to pure NaF (a_o = 4.635 Å) standard, with two successive oscillations on two newly prepared samples. The estimated error for the cell volume is, at best, ± 0.2 Å^3.

Results and discussion

In Table 1 the natural samples investigated in the present study, together with some of those recorded in the literature, are grouped according to locality. The identified As–Sb associations are either those determined in the present work or those reported in the original papers. As regards the classification of the fabric types, terminology redefined on the basis of published work (Van der Veene, 1925; Edwards, 1965; Ramdohr, 1980) has been adopted. The most important of the texture types are illustrated in Fig. 1.

Skinner's (1965) linear relationship between As and Sb cell volume versus composition has been used to calculate the atomic percentage of As in each of the two associated phases. As standards to enable use of this linear relationship to determine the percentage of As in the solid solutions produced after DTA experiments, one pure synthetic As sample and five different synthetic (As,Sb) compositions were prepared using the sealed evacuated silica tube technique. A complete heating and cooling DTA cycle up to 850 °C was run on these synthetic charges and the final products were examined by X-ray diffraction and reflected light microscopy, their cell volume being plotted on the cell volume–composition diagram (Fig. 2). Some of the cell volume values were slightly lower than those reported by Skinner (1965) for the same compositions; nevertheless, they are within the limits of analytical error.

The calculated atomic percentage of As in both of the associated phases and in the resulting solid solutions (Table 2), show that the Sb content of the As-rich phase of all texture types (except sample 597/18) is less than 4 at.%, while the As content of stibarsen ranges from a minimum of 52 at.% to a maximum of 58 at.%. On the other hand, the As content of the solid solutions formed after DTA treatment varies with the texture types, as described by Bernardini *et al.* (1984).

As already noted, all thermal experiments were performed in evacuated silica glass vials and, therefore, should be considered polybaric. This is the case even if, as indicated by the As-sublimation curve of Skinner (1965), the As vapour pressure up to 600 °C is lower than 1 atm.

The results of the DTA, run on 22 out of 36 samples, are reported in Table 3. The DTA traces in Fig. 3 show three main endothermic peaks in the heating curves of all samples: (i) a small and fairly smooth peak with a maximum temperature at 300–310 °C; (ii) a 'drift' from the base line, culminating in a weak peak with a maximum temperature around 560–570 °C, and (iii) a very pronounced, in some cases double, peak between 600 and 800 °C depending upon the As content of the charge. Only the third, high-temperature peak, is observed in the cooling curves. Other features appear in the DTA traces of some samples due to impurities, mainly As_2O_3.

The high-temperature DTA peaks are due to the passage from a single solid-phase to a single liquid-phase field in a binary system with complete solid solution and a temperature minimum. These results are in agreement with the isobaric sections inferred by Skinner (1965) for pressures higher than 10 atm. The lower temperature features in the DTA curves must arise from the mechanisms by which a

Table 1. Recorded occurrences of "allemontite" assemblages.

Locality	Identified As-Sb assemblages	Texture type	Reference or catalogue number (+)
Alder, Island, British Col., Canada	As + (As,Sb)	h	Holmes, 1936
Allemont, Isère, France	As + stb	m	1760 BO
" " "	As + stb	m	44844 BO
" " "	Sb (s.s.)	h	617/19 FI
" " "	As + stb	cr	618/19 FI
" " "	Sb (s.s.) + stb (tr)	d	630/20 FI
" " "	Sb (s.s.)	h	631/20 FI
" " "	Sb (s.s.)	h	1180 NA
" " "	As + stb	m	13225 NA
" " "	Sb (s.s.) + stb	c	17212 NA
" " "	As + stb	m	231/1 RM
" " "	As + stb	m	232/2 RM
" " "	As + stb	m	233/3 RM
" " "	stb + As (tr)	d	533/6 RM
" " "	As + stb	m	14834/3 RM
" " "	stb + As	d	2259 TO
" " "	As + (As,Sb)		Holmes, 1936
" " "	As + (As,Sb)	m	Kalb, 1926
" " "	As + stb	m	Ramdohr, 1980
" " "	α-As + α-Sb	m	Van der Veene, 1925
" " "	Sb + stb	m	Wretblad, 1941
Andreasberg, Harz, West Germany	As + stb	v	596/18 FI
" " " "	As + stb	v	597/18 FI
" " " "	As + stb	v	598/18 FI
" " " "	As + stb	v	599/18 FI
" " " "	As + stb (tr)	v	600/18 FI
" " " "	As + stb	v	601/18 FI
" " " "	As + stb	v	602/18 FI
" " " "	stb + As	m	621/19 FI
" " " "	As + stb	m	660/21 FI
" " " "	As + stb	v	225/2 RM
" " " "	As + stb	v	226/3 RM
" " " "	As + stb	v	4776 TO
" " " "	As + (As,Sb)	v	Kalb, 1926
" " " "	α-As + α-Sb	v	Van der Veene, 1925
Atlin, British Col., Canada	As + (As,Sb)		Holmes, 1936
" " " "	As + Sb		Walker, 1921
Bernic Lake, Manitoba, Canada	As + stb	d	Černý & Harris, 1978
Borgofranco, Ivrea, Italy	As + stb	v	14369 TO
Broken Hill, N.S.Wales, Australia	stb + Sb	c	Markham & Lawrence, 1962
Clausthal, Harz, West Germany	As + stb	v	6751 NA
Lucknow, N.S.Wales, Australia	prd + stb	d/h	Leonard et al., 1971
Münsterthal, Baden, West Germany	α-Sb + α-As	v	Van der Veene, 1925
Příbram, Bohemia, Czechoslovakia	stb + As (tr)	cr	622/19 FI
" " "	As + stb	v	17827 NA
" " "	stb + As	m/h	2263 TO
" " "	As + (As,Sb)		Holmes, 1936
" " "	As + (As,Sb)	v	Kalb, 1926
" " "	As + stb		Ramdohr, 1980
" " "	α-As + α-Sb	v	Van der Veene, 1925
Rush Lake, Manitoba, Canada	stb + Sb		Černý & Harris, 1973
Saxony, East Germany	As + stb (tr)	v	607/18 FI
" " "	As + stb	v	7197 TO
Varuträsk, Sweden	As + stb		Ramdohr, 1980
" "	Sb + stb	m	Wretblad, 1941
" "	As + stb	m	Wretblad, 1941
Unknown	As + stb	m	1753 BO
"	As + stb	m	632/20 FI

stb = stibarsen; prd = paradocrasite; h = homogeneous; cr = crownlet; d = drop-like
m = myrmekitic; c = cloudy-fashion; v = veining; tr = traces; (s.s.) = solid solution.
(+) Mineralogical Museum of the Universities of: BO = Bologna; FI = Florence; NA = Naples; RM = Rome; TO = Turin.

homogeneous solid solution is obtained from the intergrowths. It is reasonable to suggest that, while the endothermic peak at approximately 300 °C is due to an initial sublimation of As in the vials, which are at a initial pressure of 10^{-4} atm, the endothermic 'drift' from the base line is caused by the homogenization reaction which produces solid solution. In order to confirm this interpretation, high-temperature X-ray and optical studies and examination of phases obtained by quenching experiments from temperatures just higher than those of the DTA peaks were performed on some of the most characteristic associations.

The high-temperature X-ray photographs taken

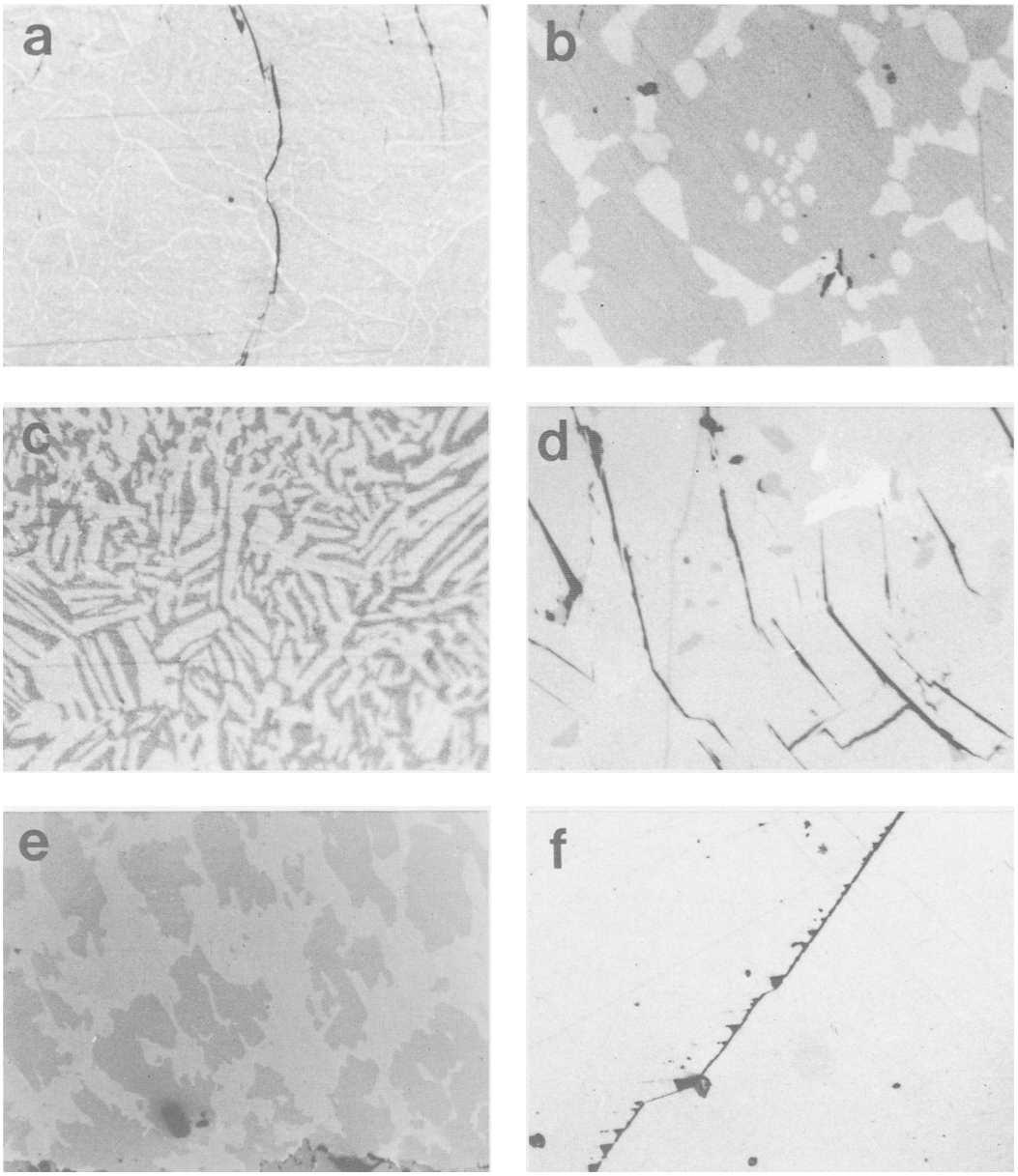

FIG. 1. Photomicrographs of natural As–Sb alloy texture types: (*a*) As-scherbenkobalt with vermiform veinings of stibarsen (white); (*b*) As with crownlet-like inclusions of stibarsen (white); (*c*) myrmekitic intergrowth between As (grey) and stibarsen (white); (*d*) drop-like inclusions of As (grey) in stibarsen (greyish-white); (*e*) Sb (s.s.) (light-grey) with cloudy-shaped inclusions of stibarsen (grey); (*f*) homogeneous Sb (s.s.). Magnifications are: (*a*) × 370; (*b, c, d, e, f*) × 230.

at 300, 400, 500 and 600 °C on a myrmekitic-type sample (632/18), while confirming the existence at 300 °C of the same phases as those at room temperature, showed at the higher temperatures only the presence of the solid solution. Optical observation of a polished section up to a temperature of 550 °C in the heating stage, even though partially obscured by the continuous sublimation

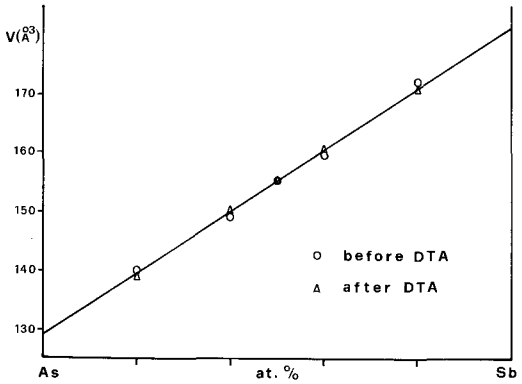

FIG. 2. Skinner's (1965) relationship between composition and cell volume of (As,Sb) solid solutions. Plots are experimental data from the present study.

of the As phase, allowed a progressive fading of the boundaries between the two phases above 300 °C to be detected, suggesting that the homogenization reaction occurs in this range of temperature. The results of the DTA experiments are plotted in Fig. 4, which shows the temperature limits between which the solid solution is formed.

To study the mechanism of the homogenization reaction and its dependence on time, two main types of quenching experiments were performed. The first involved heating samples directly in the DTA apparatus at 350, 450, and 570 °C, rapidly opening the furnace and quenching the vials in iced water. The second involved the annealing of samples in glass vials, at different constant temperatures for various periods of time followed by quenching.

The results of the first type of experiment, performed on cr-type (618/19), m-type (1760 and 660/21) and d-type (17212) samples are reported in Table 4. For all the samples the As content of the starting phases is almost constant up to 450 °C. In the X-ray diffraction patterns of the 450 °C quenched products the reflections of the solid

Table 2. Cell volumes and As at.% of natural As-Sb alloy associations before and after DTA.

Sample	texture type	Before DTA Cell volume (Å)³ As	stb	As at.% As	stb	After DTA Cell volume (Å)³ s.s.	As at.% s.s.
601/18 FI	v	129.9		98		131.2	96
596/18 FI	v	130.2		98			
597/18 FI	v	132.2		94			
598/18 FI	v	129.8		99			
600/18 FI	v	130.2		98			
602/18 FI	v	129.7		99			
225/2 RM	v	129.9	152.1	98	56		
226/3 RM	v	130.2	153.1	98	53		
4776 TO	v	130.2	151.7	98	56		
14369 TO	v	128.8	152.4	100	55		
6751 NA	v	129.5	152.0	99	56		
17827 NA	v	128.1	152.0	100	56		
607/18 FI	v	129.8		99			
7197 TO	v	131.3	150.7	96	58		
618/19 FI	cr	131.2	152.0	96	56	130.3	92
622/19 FI	cr		152.5		55	141.2	76
2263 TO	m/h	130.5	151.3	97	57	149.3	75
232/2 RM	m	128.8	150.9	100	58	142.1	75
632/20 FI	m	129.2	151.0	100	58	142.6	74
44844 BO	m	130.1	152.7	98	54	142.9	73
1760 BO	m	130.2	152.3	98	55	144.8	70
14834/3 RM	m	130.1	152.4	98	55	144.7	70
660/21 FI	m	129.9	151.6	98	57	144.9	70
231/1 RM	m	130.3	152.7	98	54	145.8	68
1753 BO	m	130.1	152.2	98	55	145.9	68
233/3 RM	m	130.3	151.9	98	56	145.9	68
13225 NA	m	129.9	151.6	98	57	146.0	67
621/19 FI	m	130.3	151.5	98	57	148.1	63
2259 TO	d	130.2	152.4	98	55	149.2	62
533/6 RM	d		151.5		57	151.2	57
		Sb(s.s.)	stb				
17212 NA	c	174.3	153.6	13	52	161.6	38
630/20 FI	d	172.4		21		148.3	59 ?
631/20 FI	h	171.9		17		172.1	17
617/19 FI	h	175.6		11		175.2	11
1180 NA	h	174.7		12		177.0	8

For abbreviations see Table 1.

Table 3. Maximum peak temperature of the thermal effects registered by DTA on heating (T°C)

Sample	Texture type	As at. % after DTA	Maximum peak temperature			
601/18 FI	v	96			810	
618/19 FI	cr	92	300	540?	705?	765
622/19 FI	cr	76	308	542	635?	715
2263 TO	m/h	75	300	567	653	675?
232/2 RM	m	75	307	525	665	708
632/20 FI	m	74	302	555	668	718
44844 BO	m	73	302	546	678	715
1760 BO	m	70	300	555	675	705
14834 RM	m	70	300	558	675	715
660/21 FI	m	70	302	560?	665	705
231/1 RM	m	68	300	560	657	695
233/3 RM	m	68	298	558	665	703
1753 BO	m	68	300	562	667	710
13225 NA	m	67	300	540?	665	695
621/19 FI	m	63	300	550	662	687
2259 TO	d	62	300	538	654	681
630/20 FI	d	59	300	538	637	655
533/6 RM	d	57	295	560	638	658?
17212 NA	c	38	296		625	
631/20 FI	h	17			620	
617/19 FI	h	11			625	
1180 NA	h	8			630	

For abbreviations see Table 1.

solution appear, but are so poorly resolved that only for sample 1760 could the As content be calculated. The composition of the solid solutions at 570 °C is identical with that of the solid solutions obtained after a complete DTA cycle. The discrepancy between these results and that of the high-temperature X-ray analysis, which at 400 °C already shows the presence of the solid solution, may be easily explained taking into account the different times for which the samples were heated.

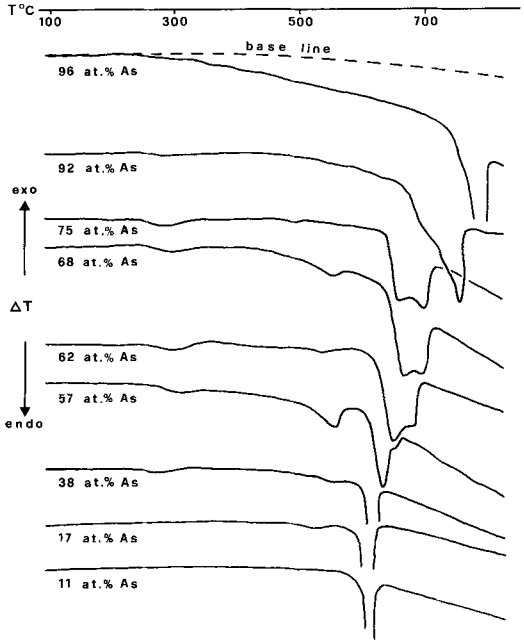

FIG. 3. DTA curves of As–Sb alloy associations of different bulk composition.

This suggests that the homogenization reaction proceeds with time.

Fig. 5 shows schematic TTT curves with rising temperature (Putnis and McConnell, 1980) for the homogenization of a sample with a myrmekitic

Table 4. As at.% in the component phases of natural As-Sb alloy samples annealed at different temperatures.

Sample	Phases	As at.%				
		Before DTA	350°C	450°C	570°C	After DTA
618/19 FI (cr-type)	As	96	96	95		
	s.s.			n.c.	89	92
	stb	56	53	49		
1760 BO (m-type)	As	98	98	95		
	s.s.			71	70	70
	stb	55	54	52		
660/21 FI (m-type)	As	98	99	98		
	s.s.			n.c.	66	70
	stb	57	53	54		
17212 NA (c-type)	Sb (s.s.)	13	16	17		
	s.s.			n.c.	33	38
	stb	52	54	46		

For abbreviations see Table 1; n.c. = not calculated.

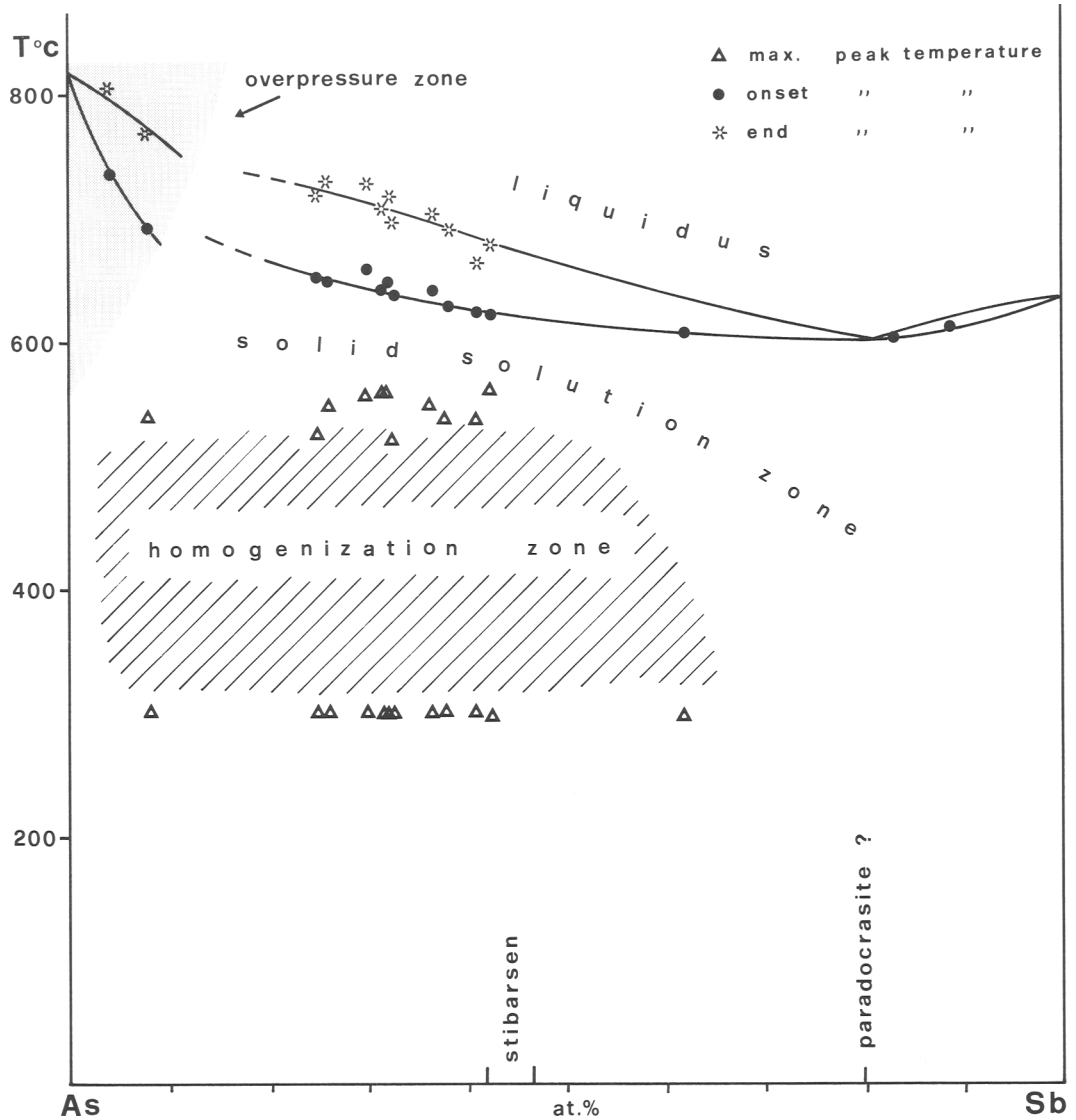

FIG. 4. Arsenic- antimony binary phase diagram showing the temperatures of peaks detected in the DTA runs.

texture (660/21) based on the constant-temperature annealing experiments. The photomicrographs in Fig. 5 emphasize the diffusion of arsenic in stibarsen which takes place along with an increase in voids in place of As lamellae. The TTT curves, marking the boundaries of different zones of textural evolution, point to a temperature of 300 °C for a complete homogenization at infinite time.

To gain further information on the homogenization reaction, a series of experiments aimed at evaluating the kinetics of the overall process was carried out. The annealing temperatures were selected on the basis of the TTT diagram of Fig. 5, considering that below 420 °C the rate of reaction would be too slow and above 520 °C too fast to be measured. The experiments were performed on sample 660/21, both because this sample is representative of the most characteristic texture type and because sufficient material showing the same texture was available. Following annealing, the quenched products were analysed by X-ray diffraction, as illustrated for the 480 °C run in Fig. 6. The

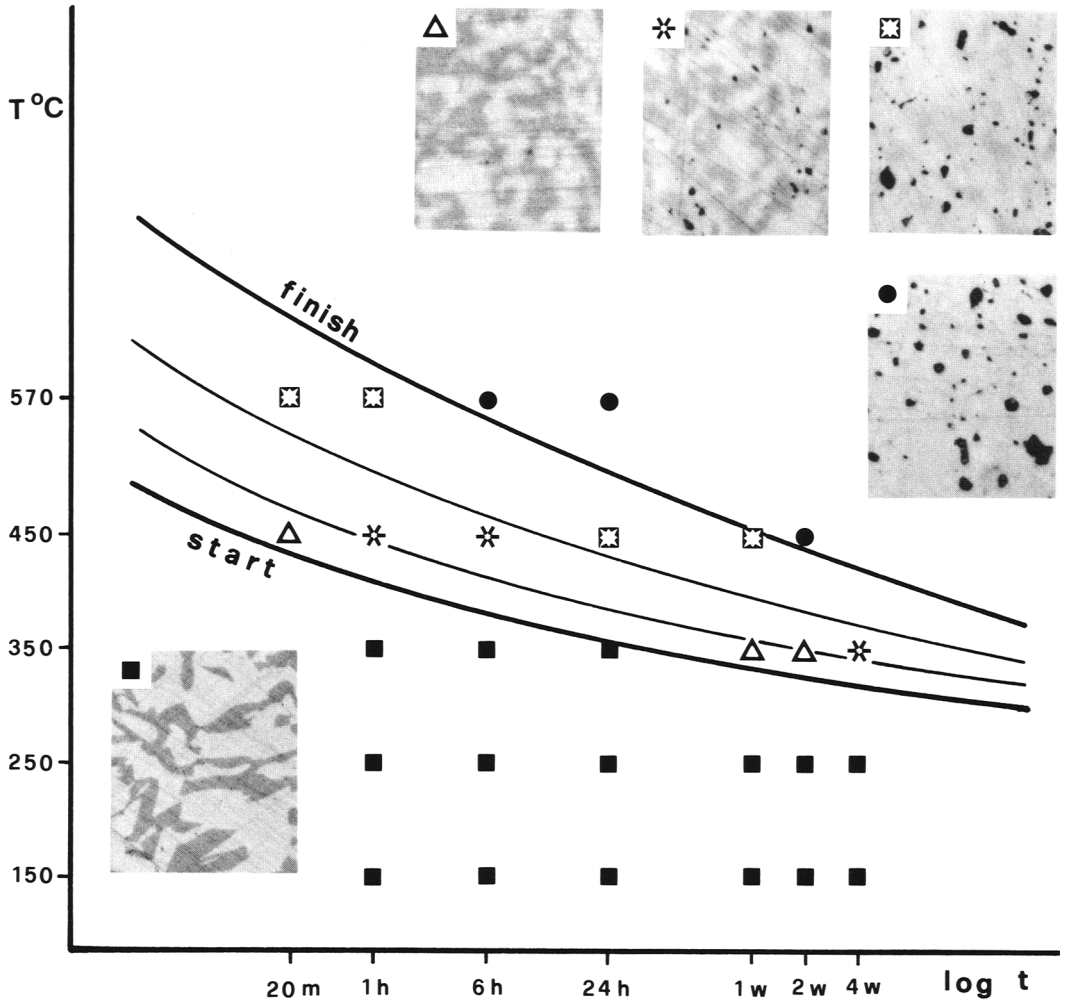

FIG. 5. Schematic TTT plots for the homogenization reaction of As–Sb alloy myrmekitic texture. In the inserted photomicrographs the boundaries between As (dark-grey) and stibarsen (greyish-white) are seen gradually fading to form an homogeneous solid solution (light-grey) with voids (black). Magnification: ×370.

progressive disappearance of the 102 reflections characteristic of As and of stibarsen coincident with the appearance of the peak characteristic of the solid solution can be easily observed. In order to evaluate the fraction (α) of the solid solution formed, the ratios between the heights of its 102 reflections at different times (and temperatures) and at the end of the reaction were determined. For the 480 and 520 °C experiments the end of the reaction was taken when the 102 reflection characteristic of the solid solution alone was present. As a first approximation the heights of the 102 reflection at the end of the reaction at 420 and 450 °C were assumed to be the same as those at the higher temperatures because the duration of the experiments did not allow a direct determination.

The data obtained were substituted into a number of kinetic equations (see Table 5, p. 74, Brown *et al.*, 1980) known to apply to various types of reactions in solids, to see if the data fit one of the equations used to define a diffusion-controlled mechanism. A relatively good fit was obtained using either the parabolic diffusion law or the Ginstling–Brounshtein equation. However, some change in diffusion mechanism apparently takes place over the investigated temperature range, and this is reflected by the change in kinetics from low (best described by the Ginstling–Brounshtein equa-

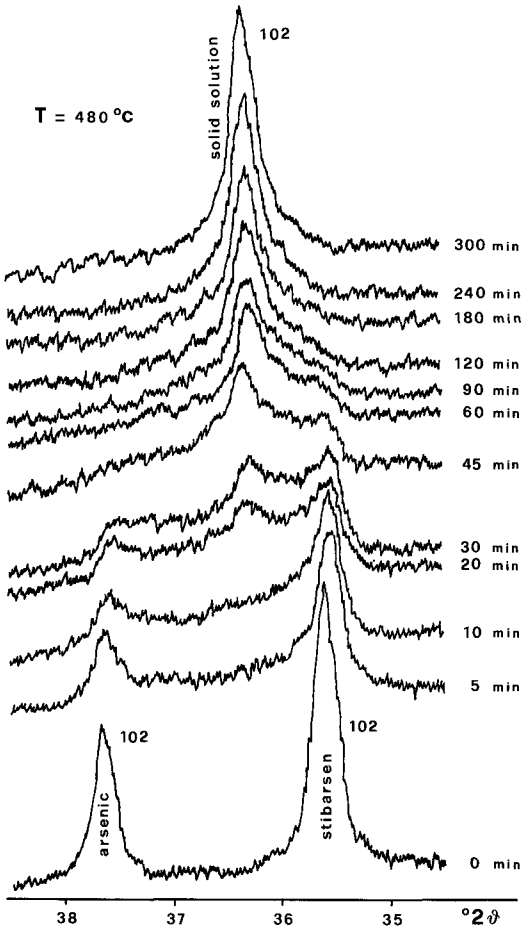

FIG. 6. X-ray diffraction patterns of an m-type As–Sb alloy heated at 480 °C for different times.

tion) to high (best described by the parabolic law) temperatures. A possible interpretation of this might involve, at higher temperatures, boundary diffusion of As from the gas phase due to its fairly high vapour pressure.

Even if homogenization reaction was by diffusion, it proved impossible to use the same rate equation at the different temperatures and, consequently, to gain information about the details of the transformation. However, a rough evaluation of overall kinetic parameters independent of the real mechanism is obtained by determining, at various temperatures, the time necessary to complete the process. In order that the ending time of the reaction could be investigated at different temperatures, the intensity ratios of the 102 reflections of stibarsen and of the solid solution are plotted as function of time in Fig. 7. In this way the ending time for 420 and 450 °C experiments could be extrapolated. No explanation has been found so far for the inflection between 180 and 300 minutes in the 450 °C run and, therefore, the relative ending time value for this run has not been used in the determination of kinetic parameters.

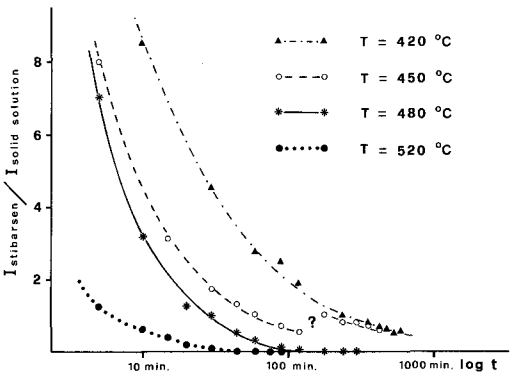

FIG. 7. Intensity ratios of 102 reflections of stibarsen and of (As,Sb) solid solution as function of annealing time at different temperatures.

The rate constants ($k = 1/t_f$) calculated from the ending time for the different temperatures have given the following values for the exponential (E_a) and pre-exponential (A) factors of the Arrhenius equation: $E_a = 37$ kcal/mol and $A = 3.07 \times 10^8$ min^{-1}. The calculated activation energy is comparable with values for metal in metal diffusion processes (see, for example, Jost, 1952) while the pre-exponential factor appears rather low when compared with the frequencies of reticular vibrations (Brown *et al.*, 1980). This led to an evaluation of the kinetic parameters in terms of the transition state theory (Glasstone *et al.*, 1941) as ΔH^* and ΔS^* using the equation

$$1/t_f = \frac{kT}{h} \exp(\Delta S^*/R) \exp(-\Delta H^*/RT)$$

and plotting $\ln 1/t_f T$ *vs.* $1/T$. This procedure gave the following values: $\Delta H^* = 36.5$ kcal/mol and $\Delta S^* = -31$ e.u.

The relatively large negative value of the activation entropy accounts for the low value of the Arrhenius pre-exponential factor. Thus, it appears that the rate determining step of the process is characterized by a rather ordered (or rigid) transition state. Unfortunately, up to now the rate determining step has not been identified.

In order to gain further insight into the kinetics, a preliminary isothermal experiment was performed on sample 660/21 which was kept at 480 °C in the cell of the TA 2000C apparatus for enough time to complete the endothermic transformation. Detailed kinetic analysis of this thermal curve has not yet been completed, but it appears that the enthalpy change connected with the endothermic reaction is of the order of 15 kcal/mol. Taking into account this value for the enthalpic change (ΔH) associated with the reaction at 480 °C, ΔS should be approximately 20 e.u. for equilibrium at this temperature. If ΔH and ΔS remain approximately the same on lowering the temperature to 25 °C, the entropy term in the equation $\Delta G = \Delta H - T\Delta S$ may well become lower than the enthalpy term and, thus, the reaction should be reversed. However, unmixing of the solid solution is not achieved in synthetic studies, possibly because of the low probability of the rate-determining step of the overall reaction. As exsolution clearly does take place in nature, the process may be made possible only by the presence of catalysts, as suggested by Wretblad (1941) and Bernardini *et al.* (1984).

Conclusions

The results of heating experiments performed on different types of natural As–Sb alloy associations confirm the high-temperature phase relations found by Skinner (1965) for the synthetic system. In the low-temperature region, the thermal effects can be correlated with an homogenization reaction between the two phases of the association to form a complete solid solution. For this reaction, a diffusion mechanism has been established but the observed variation of kinetic equations at different temperatures strongly suggests subtle changes in the mechanism for different temperature ranges. The only indications that the kinetic data provide about the nature of the rate-determining step of the homogenization reaction is that it must be characterized by a rather low probability.

Acknowledgements

The authors wish to express their thanks to the Directors of the Italian Mineralogical Museums who kindly provided the 'allemontite' samples and to Dr David J. Vaughan of the University of Aston in Birmingham for his critical reading of the manuscript.

References

Bernardini, G. P., Cipriani, C., Corsini, F., and Mazzetti, G. (1984) *Rend. Soc. It. Mineral. Petrol.* **39,** 649–56.

Brown, M. E., Dollimore, D., and Galwey, A. K. (1980) In *Comprehensive Chemical Kinetics* (Bamford, C. H. and Tipper, C. F. H., eds.), Elsevier, Amsterdam, **22,** 74.

Černý, P. and Harris, D. C. (1973) *Can. Mineral.* **11,** 978–84.

——(1978) Ibid. **16,** 625–40.

Edwards, A. B. (1965) *Textures of the Ore Minerals and their significance.* The Australasian Institute of Mining and Metallurgy, Melbourne, 50–4.

Glasstone, S., Laidler, K. J., and Eyring, H. (1941). *The Theory of Rate Processes.* McGraw-Hill, New York.

Groncharov, E. G., Cherpako, G., and Pshestamchic, V. R. (1977) *Zh. Fiz. Khim.* **51,** 2401 (Abstract in Russian).

Holmes, R. J. (1936) *Am. Mineral.* **21,** 202–3.

Jost, W (1952) *Diffusion in solids, liquids, gases.* Academic Press Inc., New York.

Kalb, G. (1926) *Metall und Erz* **23,** 113–15.

Kullerud, G. (1971) In *Research techniques for high pressure and high temperature* (Ulmer, G. C., ed.) Springer, New York, 289–351.

Leonard, B. F., Mead, C. W. and Finney, S. S. (1971) *Am. Mineral.* **56,** 1127–46.

Markham, N. L. and Lawrence, L. J. (1962) *Austral. Inst. Min. Met. Proc.* **201,** 43–80.

Parravano, N. and De Cesaris, P. (1912) *Gazz. Chim. Ital.* **42,** pt. 1, 341–5.

Putnis, A. and McConnell, J. D. C. (1980) *Principles of Mineral Behaviour.* Blackwell, Oxford.

Ramdohr, P. (1980) *The Ore Minerals and their Intergrowths* (2nd ed.) Pergamon Press, Oxford, 365–74.

Skinner, B. J. (1965) *Econ. Geol.* **60,** 228–39.

Trzebiatowski, W. (1939) *Z. anorg. allg. Chem.* **240,** 142–4.

——and Bryjak, E. (1938) Ibid. **238,** 255–67.

Van der Veen, R. W. (1925) *Mineragraphy and ore deposition,* **1,** The Hague, 70–4.

Walker, T. L. (1921) *Am. Mineral.* **6,** 97–9.

Wretblad, P. E. (1939) *Z. anorg. allg. Chem.* **240,** 139–41.

——(1941) *Geol. För. Förh. Stockholm* **63,** 19–48.

[*Manuscript received 27 February 1986; revised 9 June 1986*]